D-T Magnetic Fusion Reactor

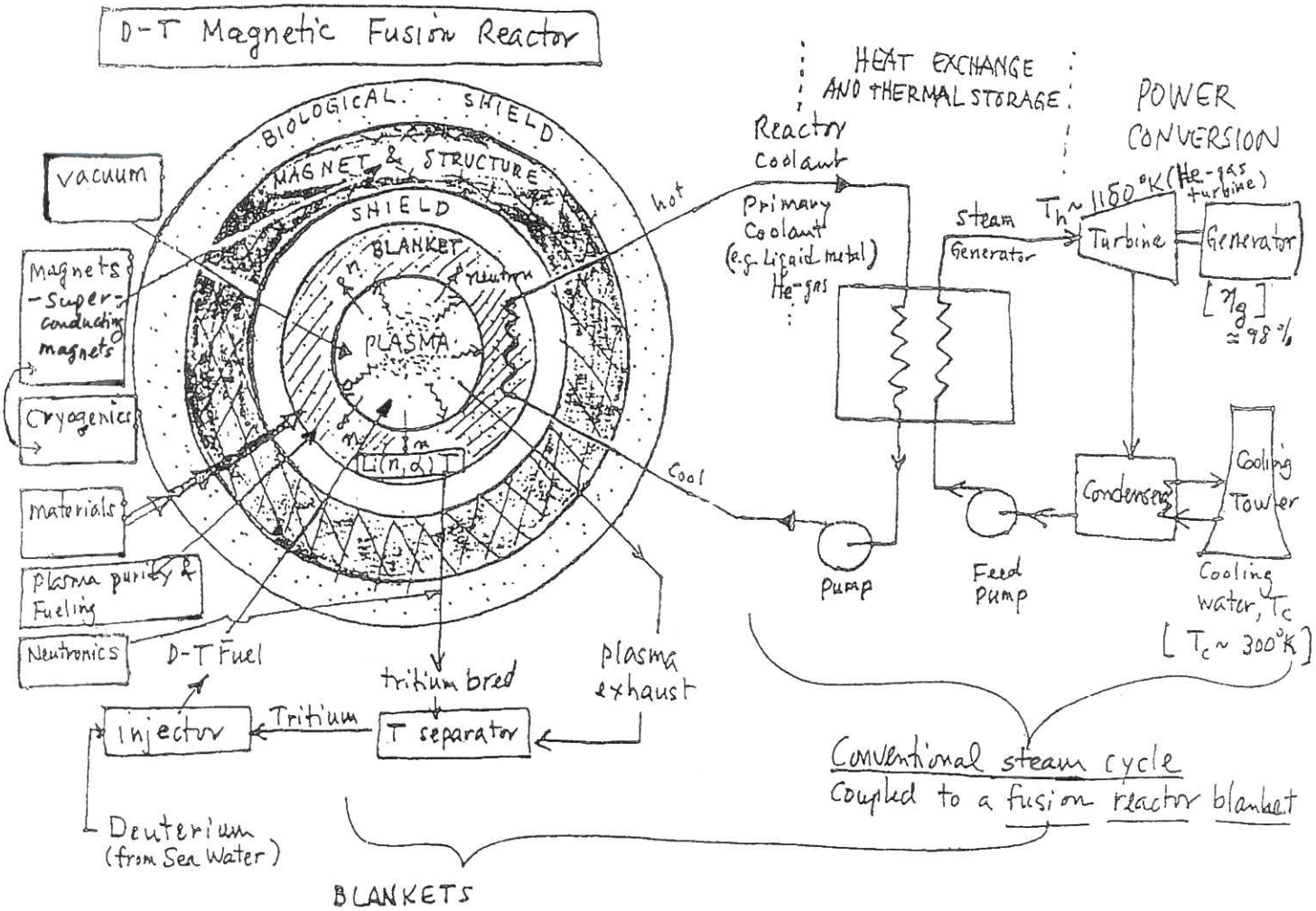

Blanket Designs

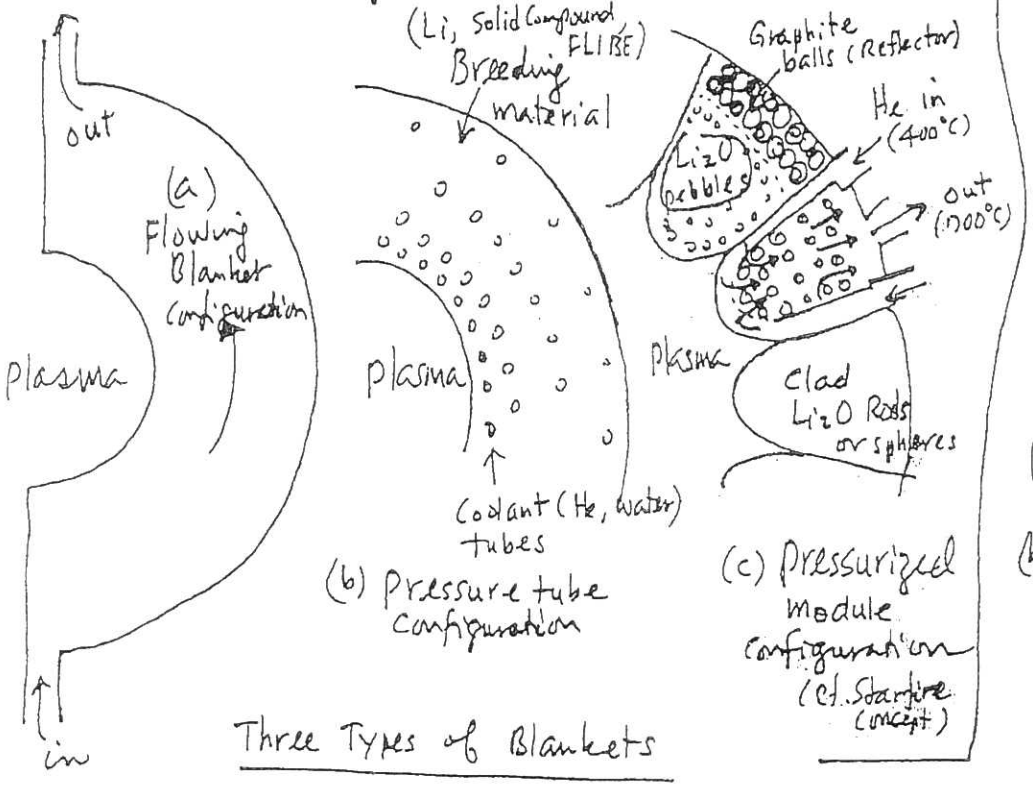

Three Types of Blankets

(a) For Li, direct the flow along $\vec{B}$ to reduce pumping power
- high thermal recirculation is problem due to high thermal conductivity of Li

(e.g. UWMAK III, WITAMIR-I) ch. 18 D

(b) NUMAK uses $Li_{62}Pb_{38}$ breeding material cooled by boiling water at 590°K, 1250 psi (8.6 MPa)

Also, STARFIRE uses water coolant with Li Al O_2 breeder

a) Flowing Blanket Configuration :

Tokamak Blanket { Coolant : Li
1st wall : TZM }

Li header will insulate hot exit Li from cooler incoming Li.

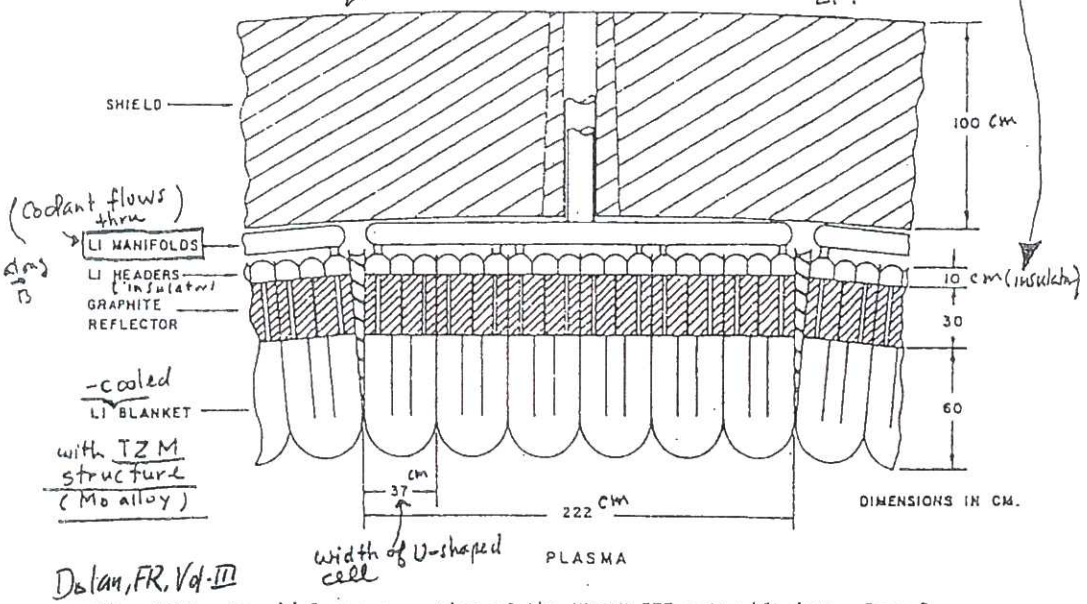

Dolan, FR, Vol-III

Fig. 2622. Toroidal cross section of the UWMAK-III outer blanket. From B. Badger et al, "UWMAK-III, a noncircular tokamak power reactor design", EPRI ER-368 (1976), Fig. VI-8-1, p. 6-8.

Note: { $\Delta T \sim 330\,^{\circ}K$
Coolant duct ~ 0.5 m
Press. drop, $\Delta p \sim 0.8$ MPa
Pumping power, $P \sim 2$ MW

Tandem Mirror Blanket { Coolant; $Li_{17}Pb_{83}$
1st wall; HT-9 }

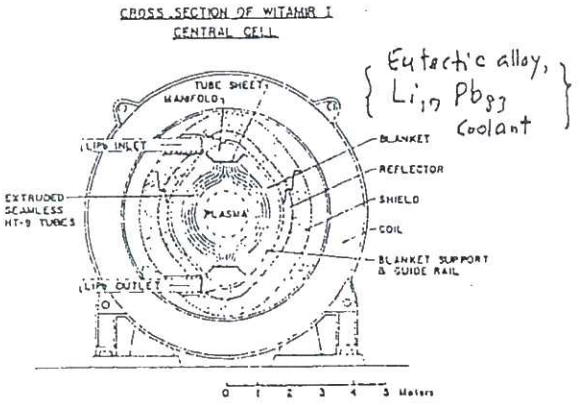

{ Eutectic alloy, $Li_{17}Pb_{83}$ Coolant }

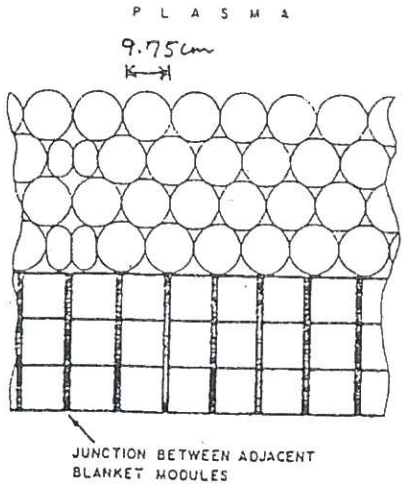

Used ferritic "HT-9" for structural(*) steel material due to good radiation damage resistance.

$\Delta T \sim 170\,^{\circ}K$

Fig. 18D5. Cross section of the WITAMIR-I blanket tubes, showing a junction between modules. From B. Badger et al, UWFDM-400 (1980), Fig. II-E-2, p. II-17.

18C. A Tokamak Reactor Design

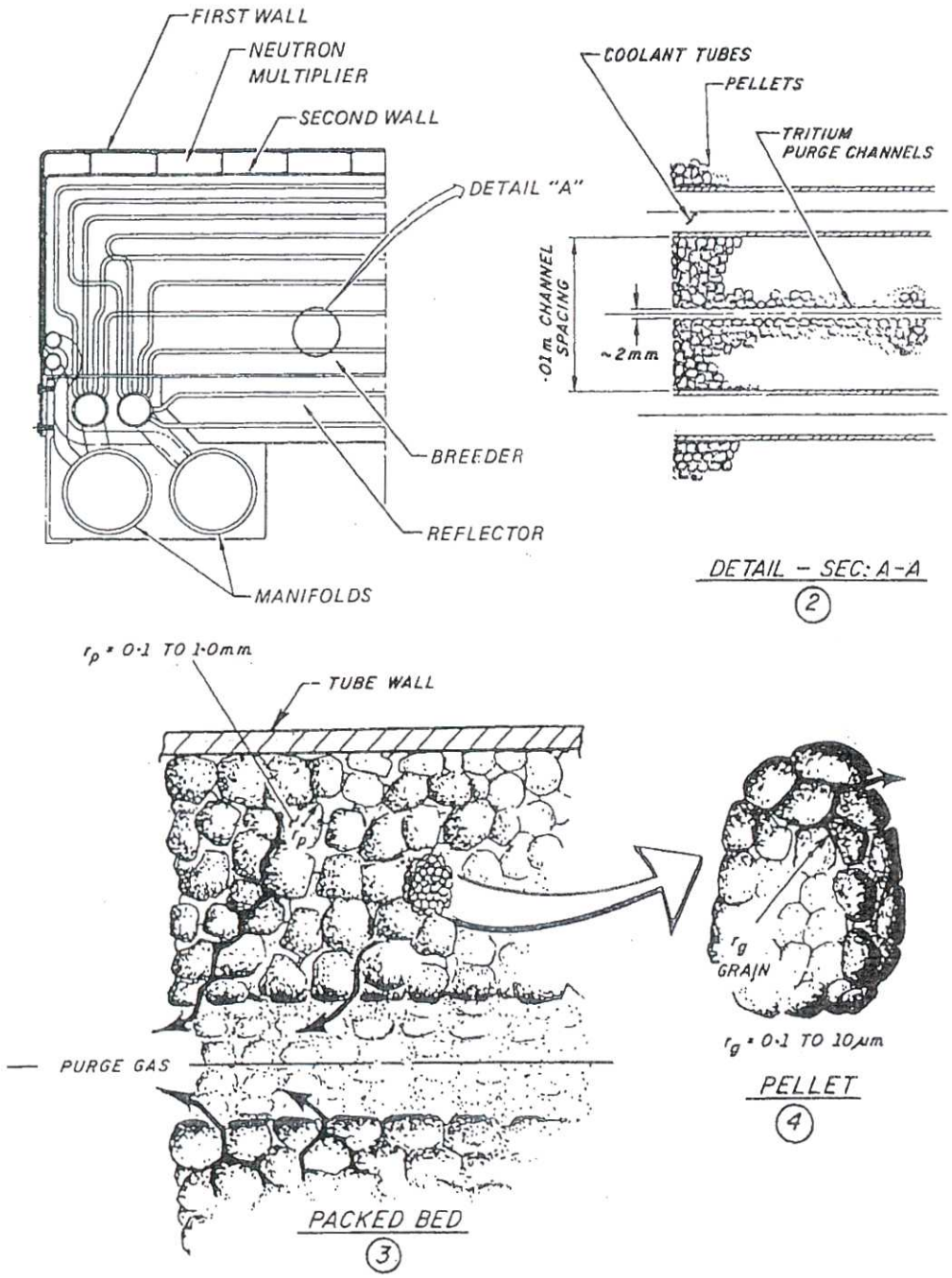

Fig. 18C3. Schematic diagram of STARFIRE blanket concept showing solid breeder microstructure with bimodal pore distribution and tritium removal scheme. From C. C. Baker et al, ANL/FPP-80-1 (1980), Fig. 2-9, p. 2-44.

The pressurized water coolant from the blanket flows to a steam generator, and the rest of the steam cycle is similar to that of a conventional pressurized water reactor (PWR) power plant. The net plant efficiency = 1200 MW/4000 MW = 30 % is limited by the low outlet temperature of the primary coolant. Other

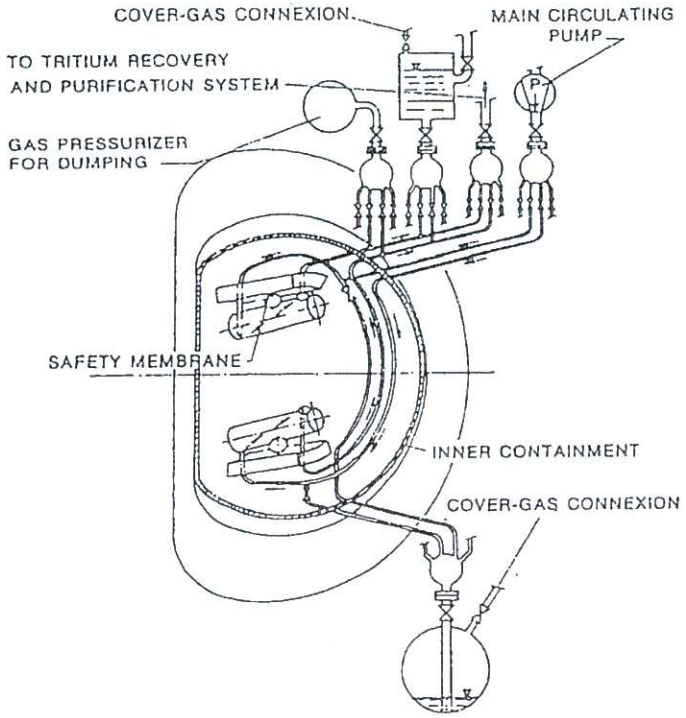

FIGURE 9 - FINTOR-D Lithium Circulation System

(Frascati Ispra Naples Tokamak Reactor)

[Ref: C. Ponti, et al., 8th Symp. on Engng Prob. in Fusion Research San Francisco (1979)]

TABLE VIII - FINTOR-D Blanket Parameters

Total wall loading (MW/m^2)	1.70
Neutron wall loading (MW/m^2)	1.36
First wall	
- total neutron flux ($n/cm^2 s$)	5.6×10^{14}
- fast neutron flux (0.8 MeV)($n/cm^2 s$)	2.5×10^{14}
- neutron damage (dpa/y)	20
- helium production (ppm/y)	300
- hydrogen (ppm/y)	750
Energy amplification in blanket	1.16
Maximum power density in the lithium (W/cm^3)	5
Heat deposition (MW/m)	
1st row	0.64
2nd row	0.21
Coolant temperatures (^oC)	
1st row inlet	200
outlet	400
2nd row inlet	400
outlet	460
Coolant pressure (bar)	50
Dimensions (cm)	
- Vessel unit inner diameter	48
thickness	0.4
- Cooling Tubes inner diameter	1.2
thickness	0.1
Length of cooling tubes (m)	5
Number of cooling tubes (m^{-1})	44
Coolant velocity (m/s)	33
Mass Flow (kg/m s)	0.73
Average Lithium Temperature (^oC)	
- 1st row	450
- 2nd row	500
Maximum wall temperature (^oC)	
- 1st row	550
- 2nd row	500
Maximum wall stress (MPa)	105

b) Pressure Tube Configuration :

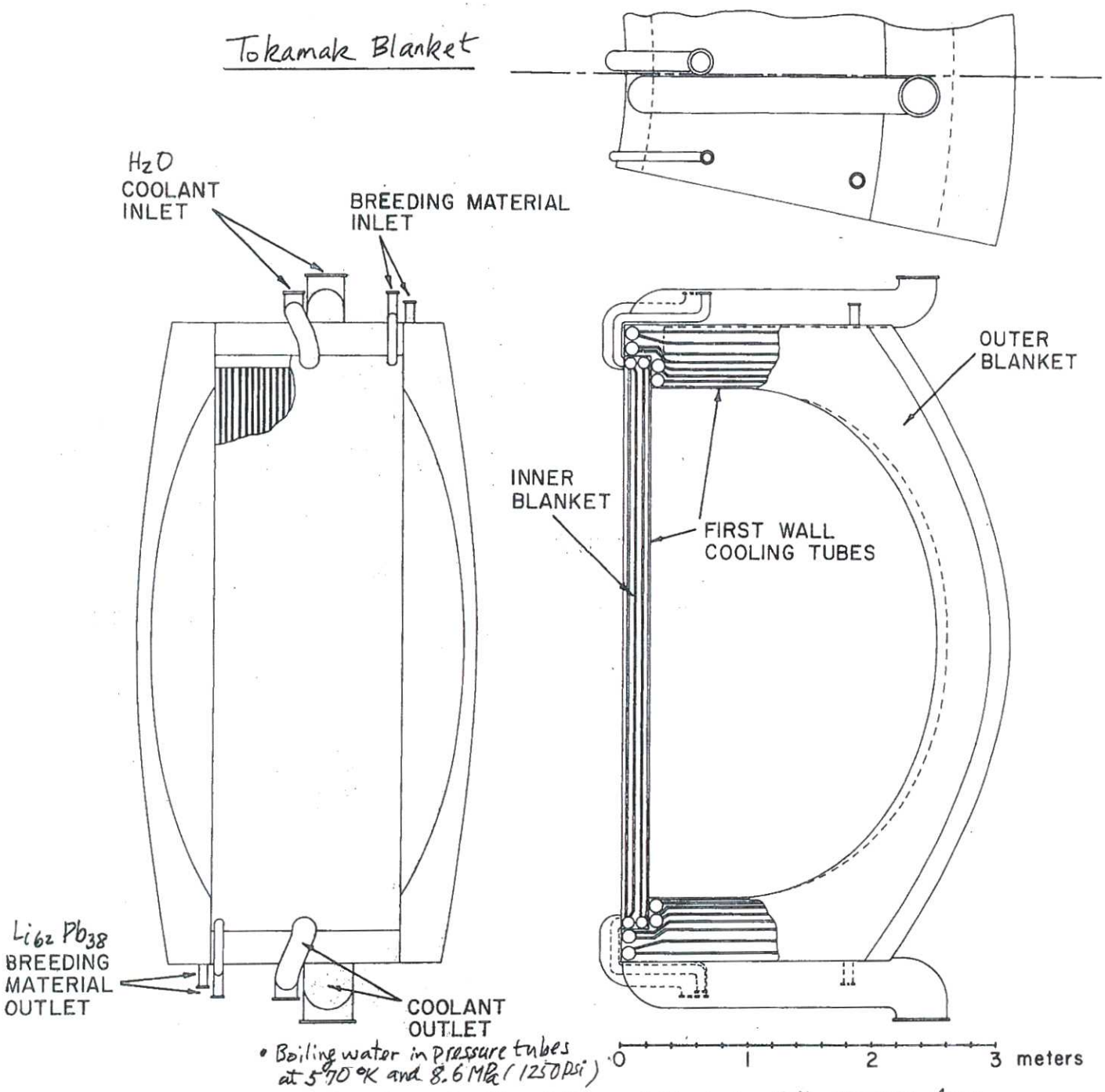

Fig. VII-C-1. Cross-Sectional View of Blanket of the NUMAK design. From B. Badger, et al., "NUMAK, a tokamak reactor design study," UWFDM-330 (1979).

c) Pressurized Module Configuration :

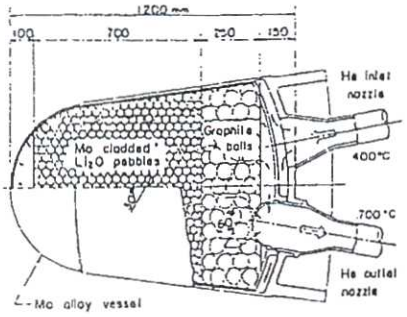

Fig. 26F4. Cutaway view of a blanket module containing pebbles of Li_2O and graphite. From A. P. Fraas, ORNL-TM-1999 (1978), Fig. 15.

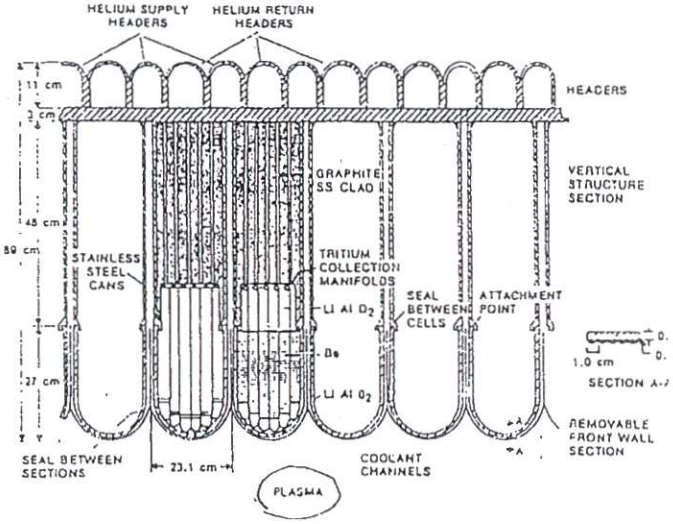

FIGURE 13 - UWMAK-II - Blanket Section

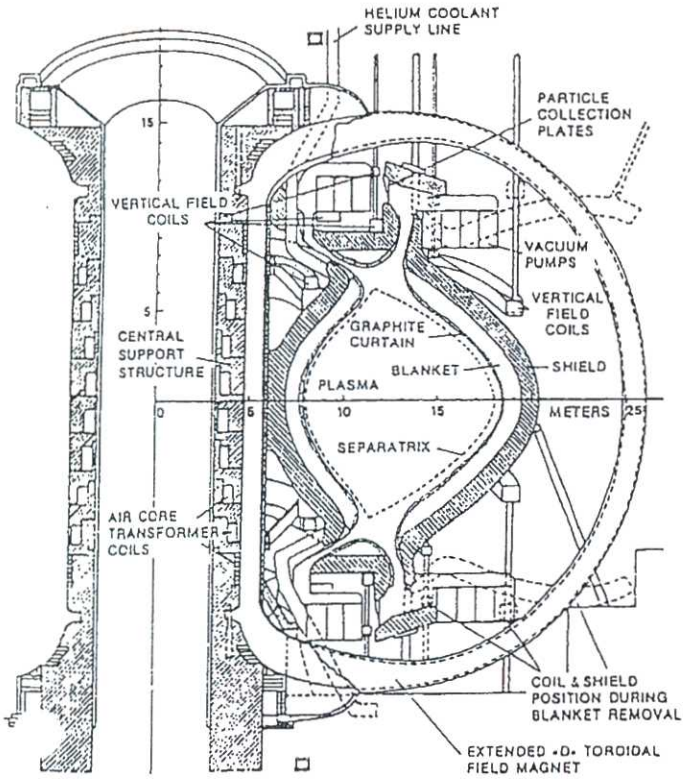

FIGURE 12 - UWMAK-II - Cross Section View

TABLE X - Properties of UWMAK-II Blanket and Shield

Thermal Power	5000 MW(t
Electric Power	1700 MW(e
Power (blanket)	4232 MW(t
Power (shield)	52 MW(th)
Structural Material	316 SS
Max. dpa rate in 1st wall	17 y^{-1}
Max. He production rate in 1st wall	292 appm y
Max. Wall erosion rate	0.15 mm y
Anticipated first wall life	2 years
First wall temperature (max.)	550°C
Max. structure temperature	654°C
Carbon curtain temperature	900°C
Max. dpa rate in curtain	5 y^{-1}
Lithium inventory in blanket	8×10^4 kg
T_2 inventory in blanket	42.0 g
T_2 leakage rate	2.0 Ci/d
Coolant	helium
Max. pressure drop	32 psi
Helium flow rate	4300 kg/s
Coolant pumping power	300 MW(e)
Coolant inlet temperature	450°C
Coolant outlet temperature	650°C
Breeding ratio	1.19
Energy per fusion	21.56 MeV
Energy attenuation to magnets	6×10^{-8}

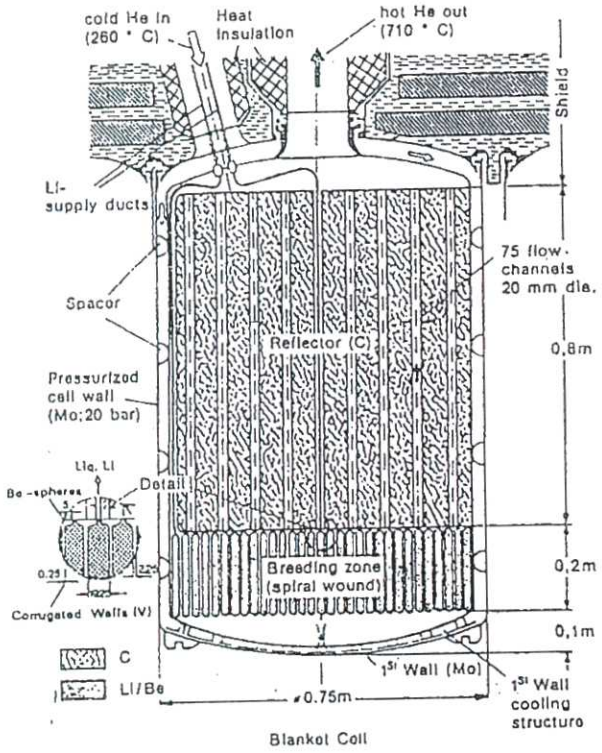

FIGURE 11 - KFA-Jülich - Blanket Cell

TABLE IX - KFA-Jülich Blanket Design

BLANKET	
Structure	Cylindrical Cells
Cylindrical Cell, outer diameter (m)	0.75 (0.7 for 10% of the cells)
Number of Cells in total	1296
Number of Cells per Segment	54
Averaged Blanket thickness (m)	1.0
Breeding Zone thickness (m)	0.2
Reflector thickness (m)	0.8
Lost Area between Cells	
First wall side (%)	16
Shield side (%)	40
Thermal Power of a Cell (MW)	3.7
Helium Coolant	
Pressure inlet (bar)	20
Temperature inlet (°C)	260
Temperature outlet (°C)	710
Mass Flow per Cell (kg/s)	1.58
Max. Mat. Temp. in Blanket (metals) (°C)	≤ 700
Replacement of Cells	individually
Fixing of Cells	in shield, bayonet joint
Rel. Pressure Losses in Helium (%)	3.6
REPRESENTATIVE BLANKET CELL	
Materials	
- Outer cell wall	Molybdenum
- 1st Wall cooling structure	SS
- Annular duct	SS
- Containment breeding zone	Vanadium
- Reflector	Graphite
Outer Shell diameter (m)	0.75
Wall thickness outer shell	
- Cylindrical part (mm)	3
- 1st Wall (mm)	4
Helium-Pressure Loss in Cell (bar)	0.74
Helium-Flow Velocity In/Outlet Ducts	100 m/s
Surface Area in Breeding Zone (m^2)	6.95

d) ITER Blankets :

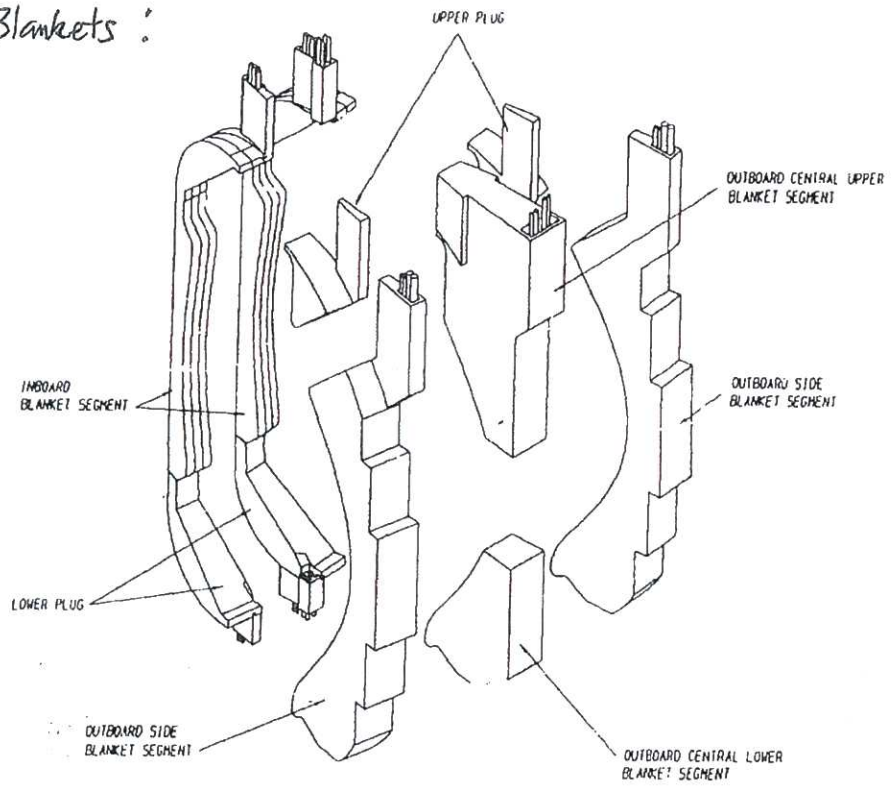

Fig. II-1. Isometric view showing the inboard and outboard blanket segments of a single sector of the ITER blanket. [Ref. D. Smith, et al., "ITER Blanket, Shield and Material Data Base," ITER Documentation Series, No. 29 (1991)]

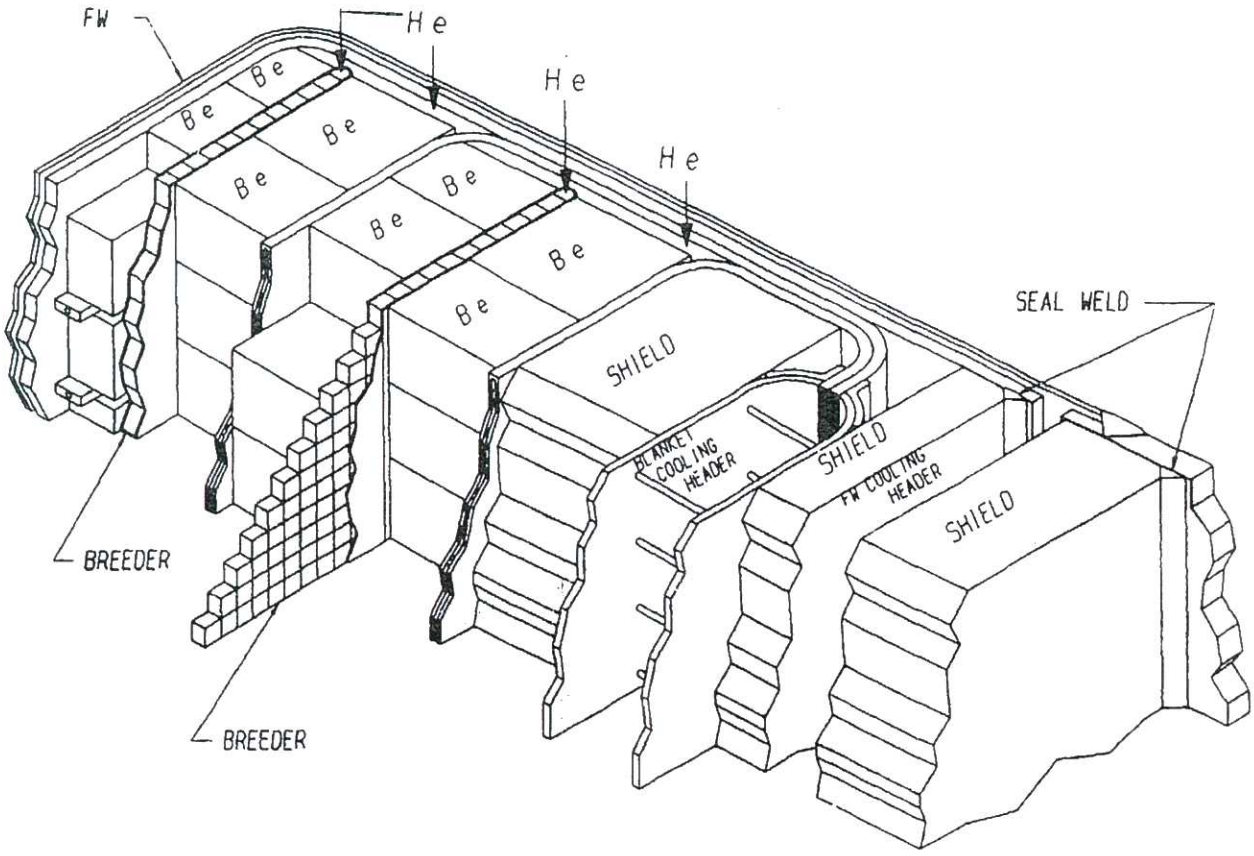

Fig. II-2. Isometric view of multilayered ceramic breeder blanket design with toroidal cooling and both Li_2O breeder and Be neutron multiplier in the form of sintered blocks

TABLE II-1. BLANKET OPERATING CONDITIONS AND DESIGN GUIDELINES (ITER)

	PHYSICS PHASE	TECHNOLOGY PHASE
FUSION POWER, MW	1100	860
NEUTRON WALL LOAD, MW/m^2 (MIN/MAX)		
INBOARD	0.4/1.1	0.3/0.9
OUTBOARD	0.8/1.5	0.6/1.2
DT FLAT BURN TIME, s	UP TO 400	2300
MINIMUM DWELL TIME, s	200	200
NUMBER OF DT PULSES	10^4	5×10^4
DT FLUENCE GOAL, MWa/m^2	0.05	3
OPERATING TEMPERATURE LIMITS,°C		
AUSTENITIC STEEL (316)		
STRUCTURAL COMPONENT		< 400
SHORT TERM OFF NORMAL		< 800
AQUEOUS INTERFACE		< 150
CERAMIC BREEDER TEMPERATURE RANGE		
Li_2O		370 - 1000*
$LiAiO_2$		450 - 900
Li_2ZrO_3		370 - 1000
BERYLLIUM		< 600

* Special attention should be given to avoid mass transport above 800°C.

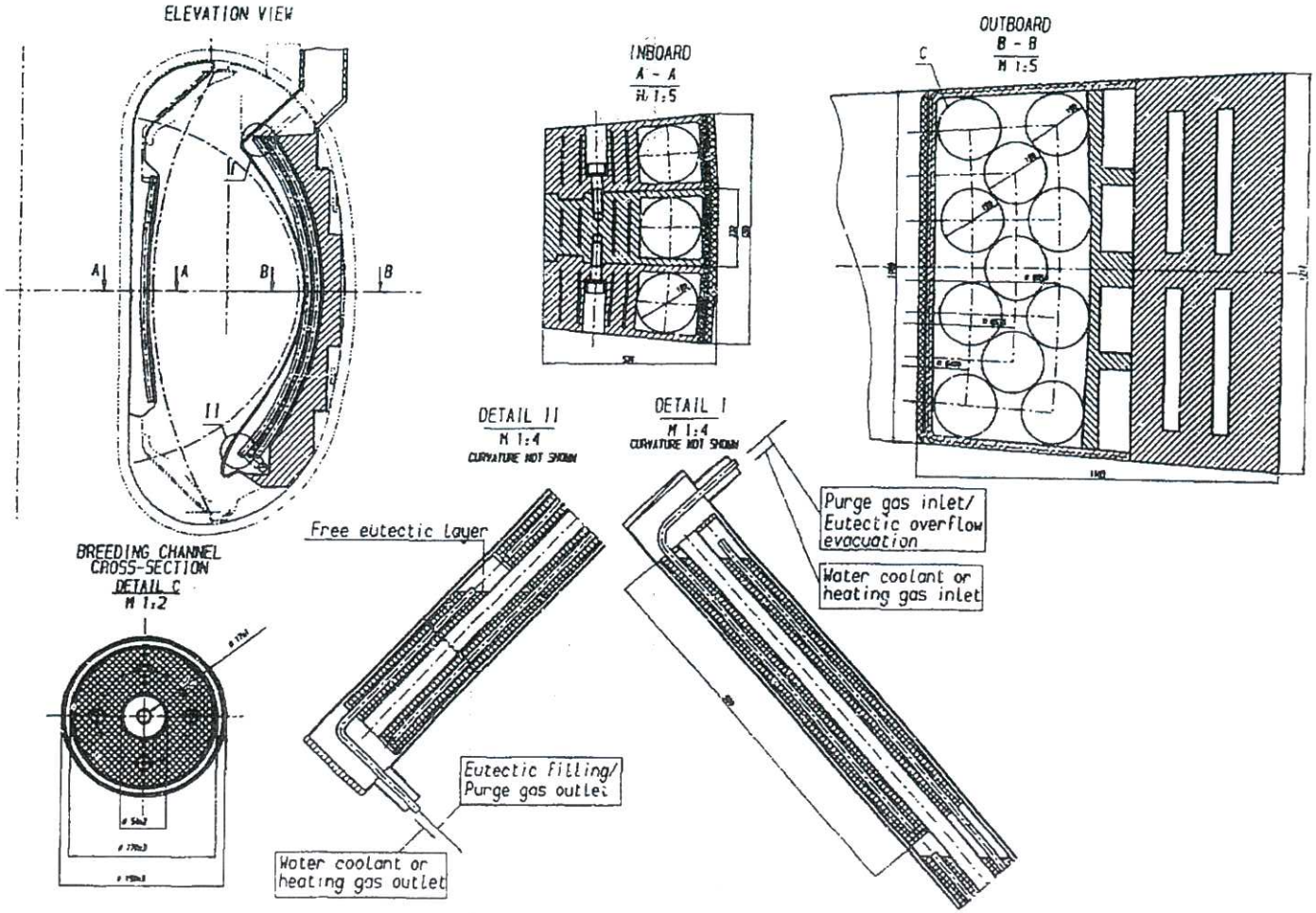

Fig. II-5. Cross sectional view of 83Pb-17 Li breeder blanket design with breeder-in-tube configuration and poloidal cooling — BIT concept.

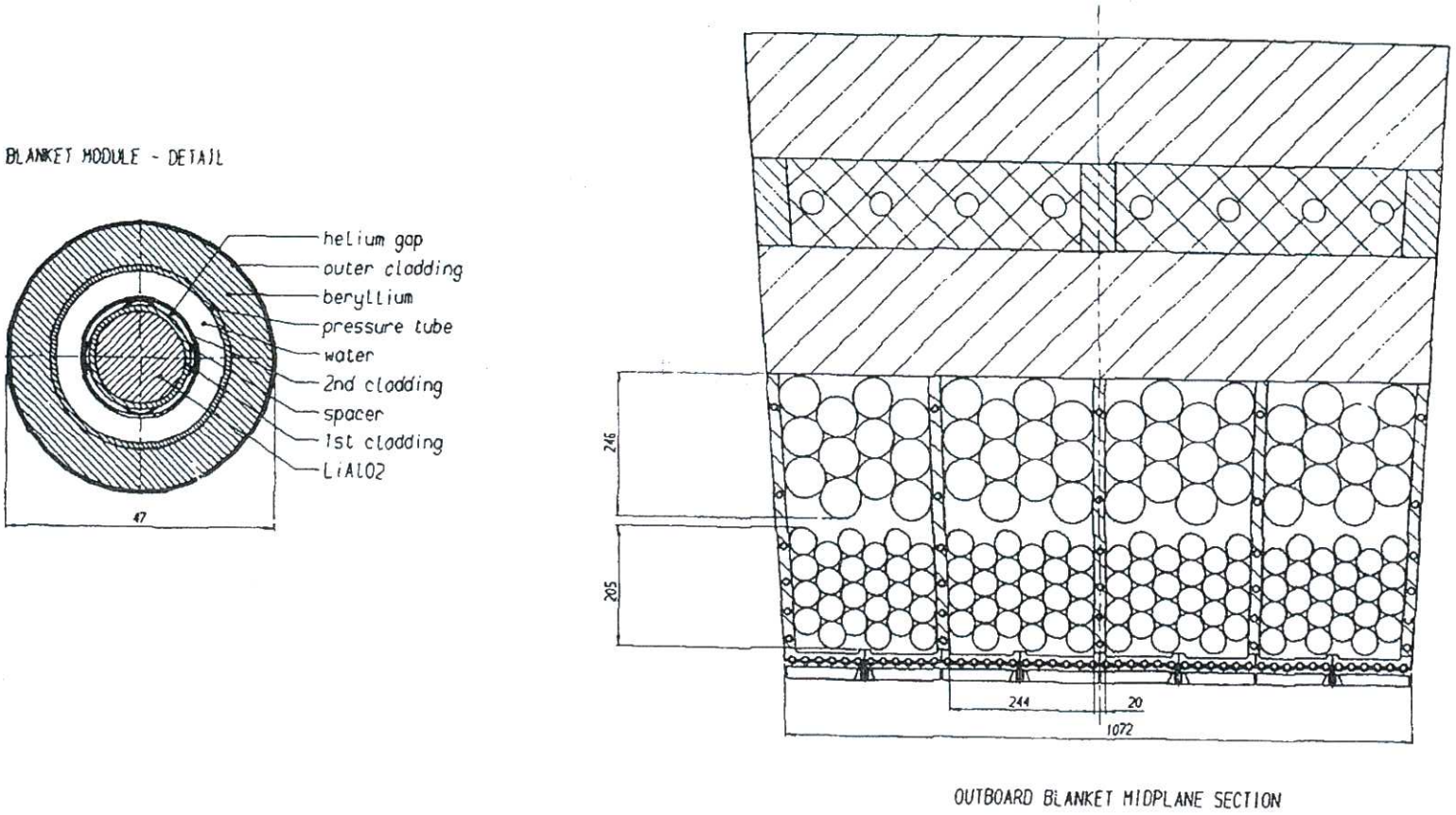

Fig. II-4. Cross sectional view of BIT ceramic breeder blanket design with poloidal cooling and both $LiAlO_2$ breeder and beryllium in the form of sintered pellets [Note : BIT = Breeder-in-Tube]

TABLE VII.1-3 THREE DIMENSIONAL TRITIUM BREEDING RATIO FOR DIFFERENT BLANKET VERSIONS WITH DIFFERENT DATA BASE

Data Base	ENDFB-IV	ENDF/B-V	
Blanket Configurations	3-D Estimation	3-D Estimation	3-D Calculation
Two breeding zones with Li_2O blocks	0.90	0.84	0.81
Three breeding zones with Li_2O blocks	0.98	0.92	-----
Two breeding zones with Li_2O pebbles	0.87	0.81	0.78

TABLE VII.1-7 NEUTRON BALANCE FOR THE LEAD LITHIUM BLANKET

DT neutron source	1.00		
(Pb Be) (n, 2n) - neutrons	0.42		
	Capture by zones	Tritium Breeding	local TBR
Inboard	0.27	0.13	0.69
Outboard Blanket:	0.97	0.70	1.04
Divertor Regions	0.18		
TOTAL	1.42	0.83	

[Ref. D. Smith, et al., ibid.]

CANDIDATE MATERIALS

Component	Candidate Materials
Structural Materials	
First Wall/Blanket	Type 316 austenitic steel (SA) Type 3/6 austenitic steel (CW) MN stabilized austenitic steel
Divertor	Copper Alloys Molybdenium Alloys Niobium Alloys
Tritium Breeding Materials	
Ceramic Breeder	Li_2O $LiAlO_2$,Li_4SiO_4,Li_2ZrO_3
Metal Breeder Materials	83Pb-17Li eutectic Alloy
Aqueous Lithium Salt Breeder	$LiOH$,Li_2NiO_3 (solutions)
Neutron Multipliers (n, 2n)	Beryllium Lead
Plasma Facing Materials	
Carbon based Materials	Nuclear grade carbons pyrolytic graphite carbon fiber composites
High-Z coatings	Tungsten
Low-Z coatings	Beryllium
Ceramic Insulators	
Oxides	Al_2O_3, $MgAl_2O_4$,BeO
Nitrides	AlON,Si_3N_4,

Ref: D. Smith, et al., "ITER Blanket, Shield and Material Data Base," ITER Documentation Series, No. 29, IAEA (1991).

Materials Issues – "Revisited"

B. Mechanical Behavior (§8.3/§8.4)

Yield strength, ductility, fatigue, and thermal creep.

Definitions:

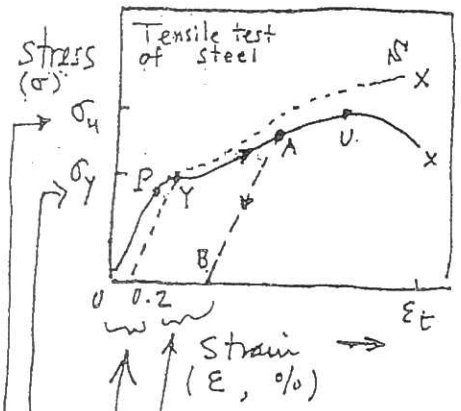

① Nominal (conventional) stress (σ) = $\frac{(\text{force})}{(\text{original X-sectional area})}$

② Strain (ε) = $\frac{(\text{change in length})}{(\text{original length})}$ (= fractional elongation)

③ Modulus of elasticity, $E = \frac{d\sigma}{d\varepsilon}$ (Young's Modulus) (along the "linear portion")

{Strain is linearly proportional to stress up to limit, P}

{At the yield stress, σ_y, plastic deformation begins (irreversible process) e.g. If load were removed at point A, the strain would follow curve A – B.}

{Ultimate stress, σ_u, is the peak conventional stress. Specimen X-sect^{n} area decreases → ∴ → stress continues to increase up to the point of failure (dashed curve O–P–S)}

④ Yield strength ⇔ stress (Pa)

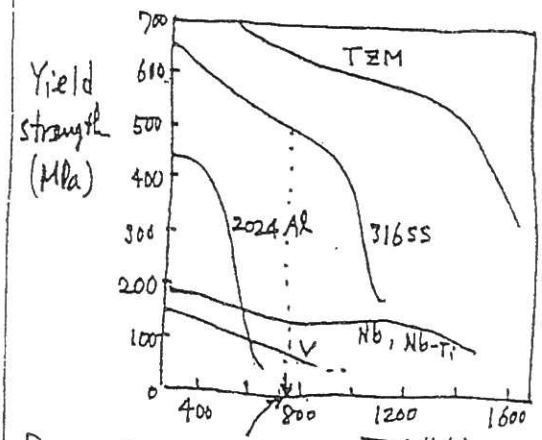

[e.g. Critical T., 670°K for 316 SS]

⑤ ductility = ability of materials to stretch before they break (e.g. rubber band has good ductility, but not in a liquid nitrogen where it becomes brittle; & it also becomes embrittled in sun's rays)

[Note: rupture = total elongation]

Measured in fractional elongation (strain)

Need 0.4 % uniform elongation for reactor components

radiation hardening ⇐ stress ↑

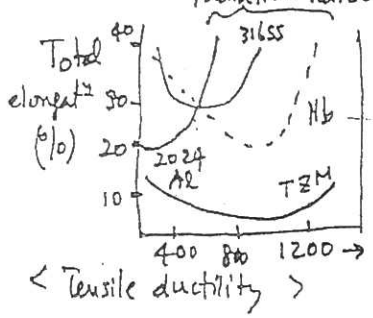

< Tensile ductility >

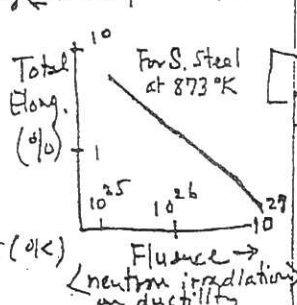

< neutron irradiation on ductility >

⑥ fatigue = "crack" growth and fracture during cyclic loading;

most difficult material problem in → e.g. (aircraft wing / bridge / steam turbine) designs!

[e.g. metal bendings for easy crack;

[e.g. Fusion reactor's stress changes when magnet coils turned on and off.

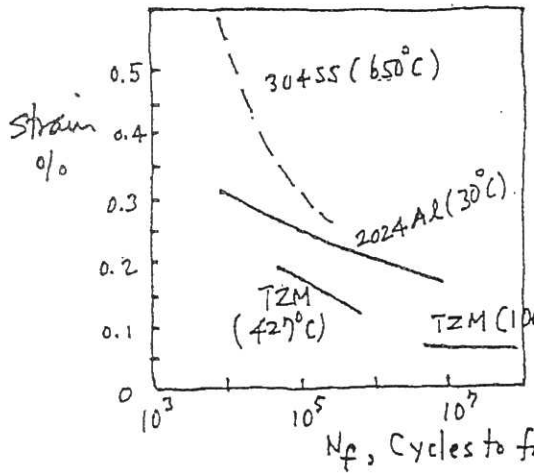

Fatigue "lives" of a few alloys

⑦ thermal creep = Gradual deformation (or yield) of irradiated metal over long periods of time ($1-10^4$ hrs ≈ 14 mos.) at $T \geq 0.5 T_m$ [melting temp.]

Note: [1 yr = 8.76×10^3 hrs]

[e.g. If stress is applied for long time the metal will eventually rupture]

time; $\tau_{creep\ rupture} \sim$ Stress, Temp. (only in irradiated metals)

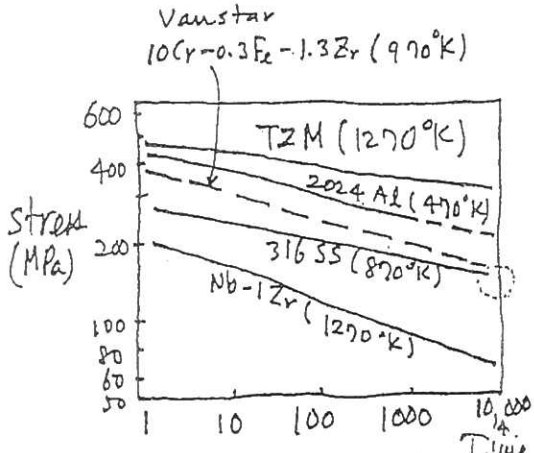

Stress causing thermal creep rupture of various alloys

e.g. Fusion reactor components should function at least this long. → should keep 316 SS (at 870°K) below 160 MPa.

In-Reactor Deformation; ⑧ swelling = increase in macroscopic dimensions due to creation of new lattice sites as vacancies precipitate as cavities.

[changes in dimensions ⇒ swelling, irrad'n creep]

[Dominant effect at $T > \frac{1}{4} T_m$] ← melting temp.

[Note: changes in mechanical behavior ⇒ radiation hardening, embrittlement, etc.]

Swelling depends on
- alloy composition (e.g., Ni content of SS-316)
- metallurgical state (e.g. cold worked SS-316 has less swelling than solution annealed SS-316)
- temperature (directly proportional)
- displacements (swelling ↑ as dpa ↑)
- helium (as He ↑, swelling ↑)

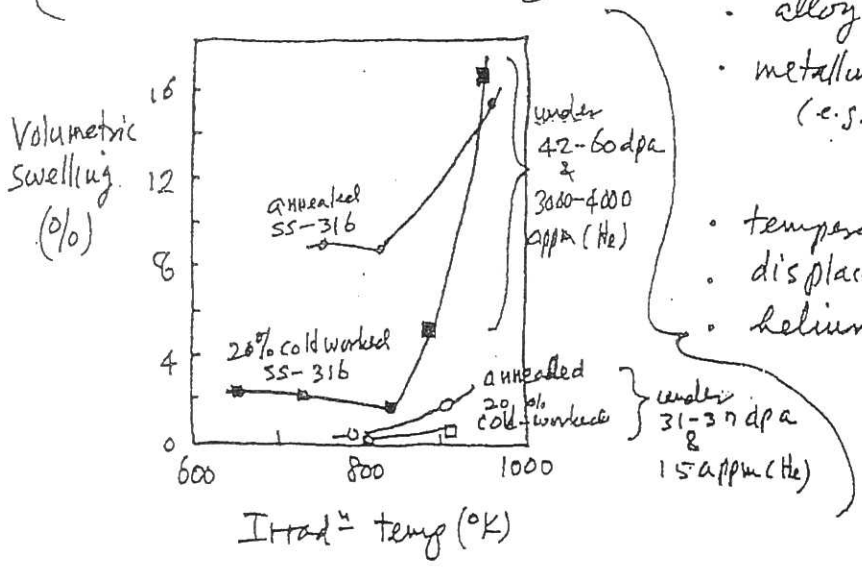

⑨ irradiation creep = change of elongation with time during static loading and irradiation

(Varies strongly w/ applied stress but weakly w/ temperature)

[f_p = pole factor; R_D = dpa/sec] → $\frac{\dot{\varepsilon}}{f_p R_D}$

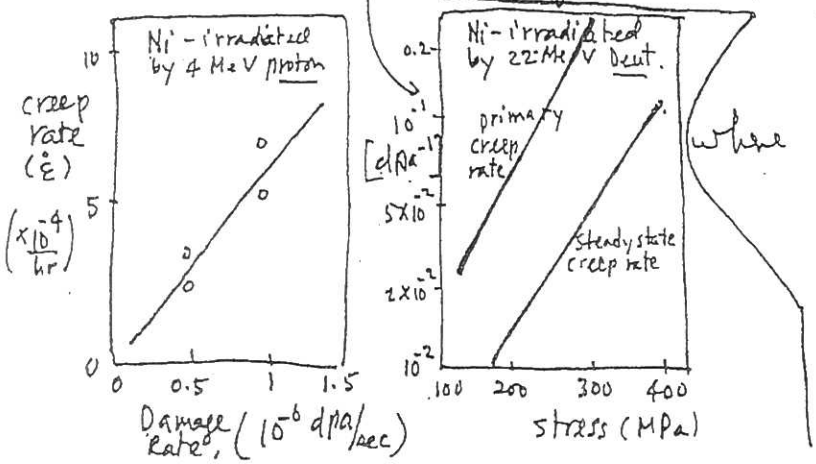

Rate of change of elongation, $\dot{\varepsilon}$,

$$\frac{d\varepsilon}{dt} = \frac{A\sigma^2 L}{\mu^2 b \cdot d} \nu_{climb}, \quad \ldots (8.10)$$

where
- A = a constant
- σ = applied stress
- L = av. spacing between "obstacles"
- μ = shear modulus
- b = Burgers vector
- d = av. height of the obstacles
- ν_{climb} = dislocation climb velocity (~ damage rate, dpa/sec)

Candidate Structural Materials

	Designation	Nominal Composition (wt.%)
1.	Type 316 SS - SA & 20 CW (Austenitic steel; — Face Centered Cubic structure	Fe - 17 Cr - 13 Ni - 2.5 Mo - 0.05 C
(2.)	PCA (Prime Candidate Alloy) (Ti stabilized 316 SS)	16.59 Ni - 14.27 Cr - 1.62 Mn - 1.96 Mo - 0.53 Si - 0.32 Ti - 0.046 C - 0.008 N - 0.04 Co - 0.014 P - 0.003 S
(3.)	HT-9 (ferritic steel; — Body centered Cubic structure)	Fe - 12 Cr - 1 Mo - 0.5 W - 0.3 V - 0.2 C
4.	TZM (a Mo alloy)	Mo - 0.5 Ti - 0.08 Zr - 0.03 C
5.	9 Cr - 1 Mo	Fe - 9 Cr - 1 Mo - 0.5 W - 0.15 V - 0.1 Nb - 0.08 C
6.	Ti - 64	Ti - 6 Al - 4 V
7.	Ti - 6242	Ti - 6 Al - 2 Sn - 4 Zr - 2 Mo
(8.)	Vanadium alloy	V - 15 Cr - 5 Ti

Blanket Concepts :

Breeder	Coolant	First Wall / Structure
Li_2O	He	HT-9
$LiAlO_2$ / Be	H_2O	PCA
Li	Li	V - Cr - Ti
Li Pb	Li Pb	HT-9

Specific Materials (§ 8.8 of Dolan's MFT):

1. Beryllium – used for the first wall in ITER (due to low atomic number and reasonable mechanical and thermal properties
   – used in JET, however, its retention of tritium, low allowable temperature, and toxicity could be problems for the first wall in DEMO

2. Reduced activation ferritic – martensitic (RAFM) steels
   – one of the best candidates for fusion reactor structural material: very low swelling, suppressed He-bubble down to nanometer range, long-term industrial experience with steels up to 140 dpa, better thermal conductivity than austenitic steels (e.g., 316LN), good irradiation properties, etc. [Disadvantages – Ductile to brittle transition temperature (DBTT) decrease after irradiation at $T_{irr} < 400$ °C, upper operation temperature limited by creep strength at $T_{max} \sim 550$ °C.]

Dolan 0.2 % strain

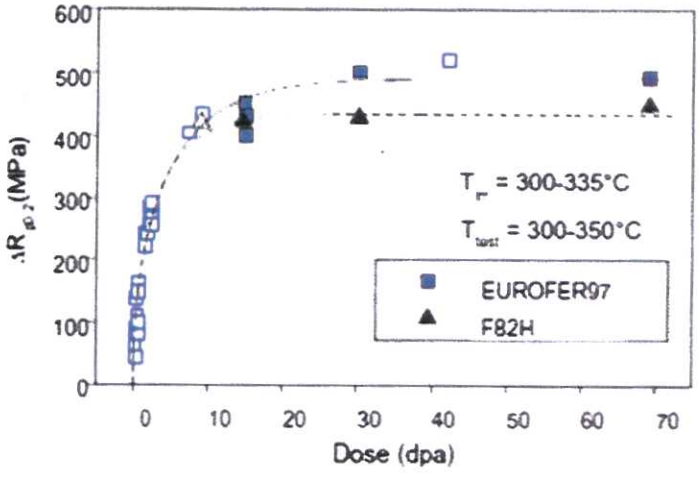

Fig. 8.29 Offset yield stress versus dose for EUROFER97 and F82H steels irradiated at 300–355 C and tested at 300–350 C. Full symbols represent BOR60 (fission reactor) experimental data, and open symbols are from previous studies. The solid line is a least square fit to the EUROFER97 data, and the dashed line is just a guide to the eye (Gaganidze et al. 2011, Fig. 1)

[Note: EUROFER97 = Fe-9Cr-1W-0.2V-0.12Ta
and F82H = Fe-8Cr-2W-0.2V-0.04Ta]

rad^n hardening & embrittlement saturate ΔDBTT saturates

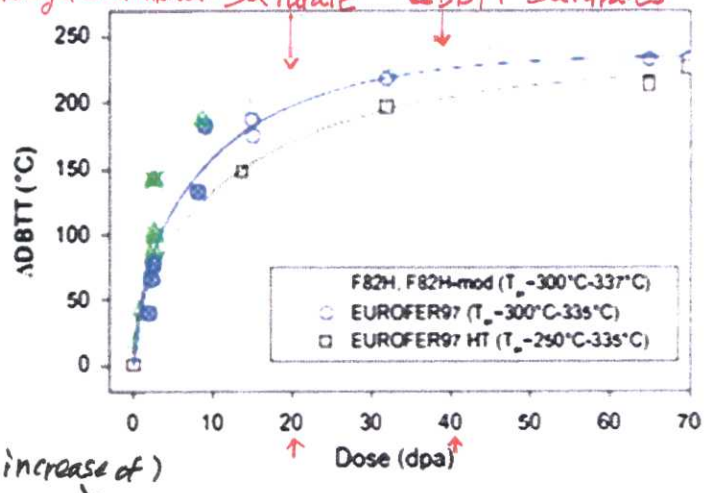

(increase of)

Dolan

Fig. 8.30 Irradiation shifts of the DBTT versus irradiation dose for EUROFER97, EUROFER97 HT, and F82H steels. The open symbols represent BOR60 experiment results and the crossed symbols are from previous studies. The solid lines are a model description of the data (Gaganidze et al. 2011, Fig. 4)

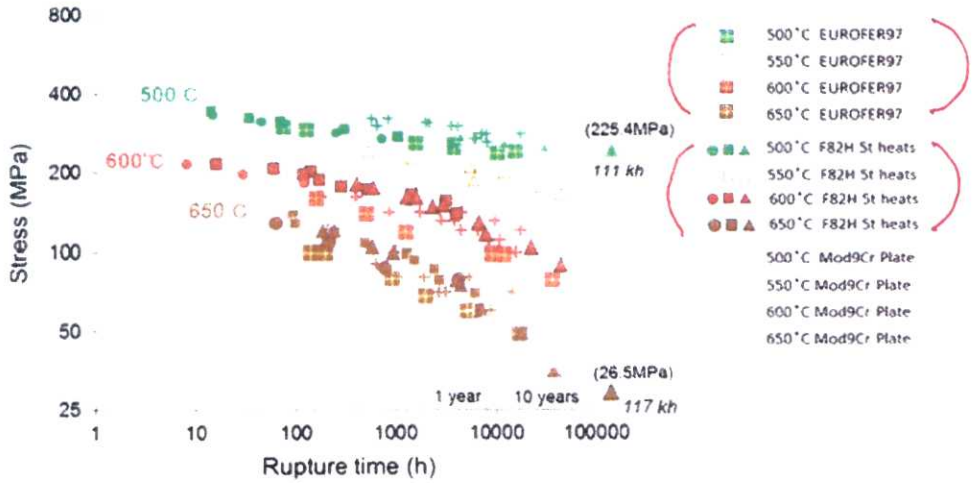

Dolan

Fig. 8.31 Creep rupture time of F82H and EUROFER at various temperatures. Mod9Cr plate data is plotted for comparison (Tanigawa et al. 2011 Fig. 4)

"produced by powder metallurgy"

3. Oxide dispersion strengthened (ODS)/ RAFM steels

– high temperature creep limit may be improved to $T_{max} \sim$ 650–750 °C.

Table 8.11 Comparison of two developmental ODS steels (Rieth 2008)

	Advantages	Disadvantages
12–16 % ODS ferritic steel	Higher temperature	Anisotropic mechanical properties
	Better oxidation resistance	Lower fracture toughness
9 % ODS martensitic steel	Nearly isotropic properties after heat treatment	Limited to T < 700 °C
	Better fracture toughness Scalable fabrication	Marginal oxidation resistance at high temperature

4. Tungsten

- tested as a wall material in JET; as divertor for ITER (minimizing tritium trapping)
- pure tungsten is very brittle; cannot be welded, just brazed by joining two metals together by melting and flowing a filler metal into the joint. Use tungsten alloys brazed on RAFM, W-2Ti-0.47 Y_2O_3 [brazing material, 55Ni-45Ti]

Dolan, **Table 8.12** Some properties of tungsten

Melting temperature	3,696 K
Density	18,950 kg/m^3
Thermal conductivity	113 W/(m K)
Poisson's ratio	0.2
Young's modulus	370 GPa
Thermal expansion coefficient	4.5 × 10^{-6} K^{-1}

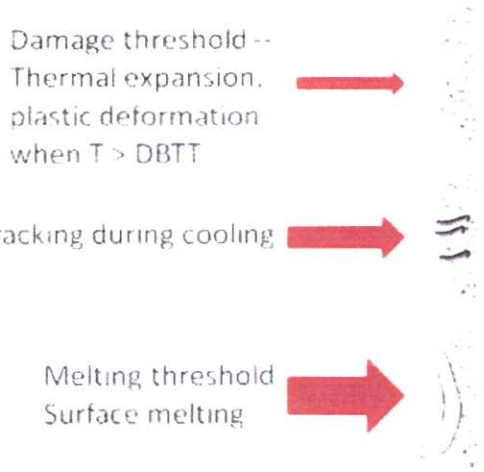

Fig. 8.32 Effects of increasing power flux (*top* to *bottom*) on tungsten surface (based on Coenen et al. 2010)

Ref. Dolan, MFT

Note: Operate W components
800°C < T < 1300°C
↑ to avoid embrittlement
↑ to avoid recrystallization

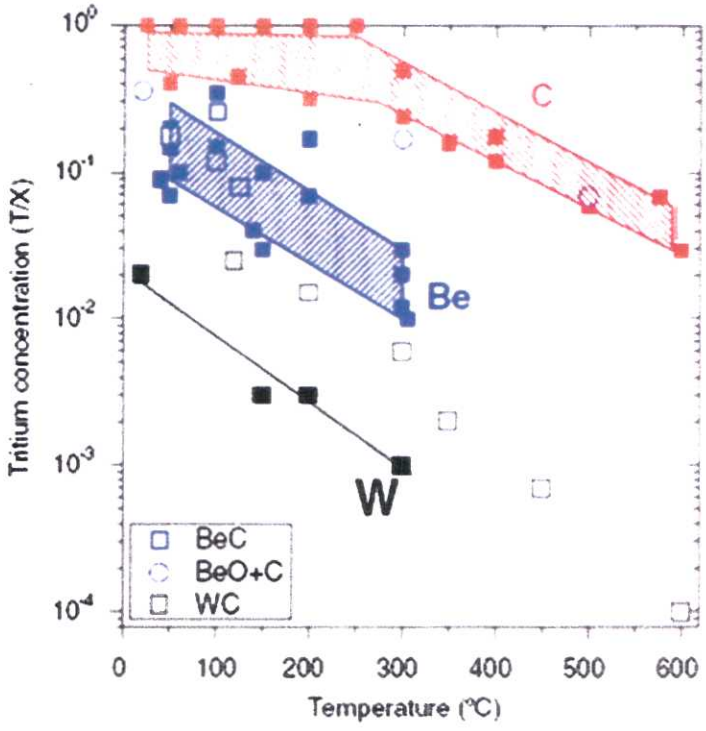

Fig. 8.33 Retention fraction of T in co-deposited C, Be and W versus Temperature (Roth et al. 2008, Fig. 4)

tungsten retains much less tritium →

5. Vanadium

- vanadium alloys are compatible with lithium coolant (e.g., up to ~700°C for V-4Cr-4Ti; ~1700°K for V-20Ti)
- annealing temperature below 1000°C to avoid embrittlement (cf. at 1100°C, Ti NOC blocks dissolve)
- a tungsten layer can be bonded to vanadium by vacuum plasma spraying or by brazing (cf. embrittlement may occur)

Maximum Temp (°K) compatible to coolant and structure:

Coolant \ Structure	316 SS	Ni-base	V	Nb	Ti
Liquid Li	770	720	1070	1270	1070
He	970	1020	< 620	< 620	670
Molten Salt	920	970	< 570	< 570	< 570
H_2O	~ 670	~ 720	< 570	< 570	< 620 (uncertain)

Similar behavior (316 SS, Ni-base); similar behavior (V, Nb)

6. Ceramics

- good for high heat flux materials in divertors, limiters, and first walls; also for insulators, for windows, for thermal insulation, and for neutron moderation and shielding.
- however, subject to fabrication difficulties, thermal stress, creep, and fatigue problems compounded by brittlement even before irradiation
- neutron irradiation can cause swelling, loss of thermal conductivity, and increased power loss in rf windows by radio waves and microwaves.

7. Graphite

- good thermal resistance, neutron reflection and moderation capability, high temperature stability, and low atomic number.
- during neutron irradiation, graphite first shrinks, then swells (see Fig. 8.34)

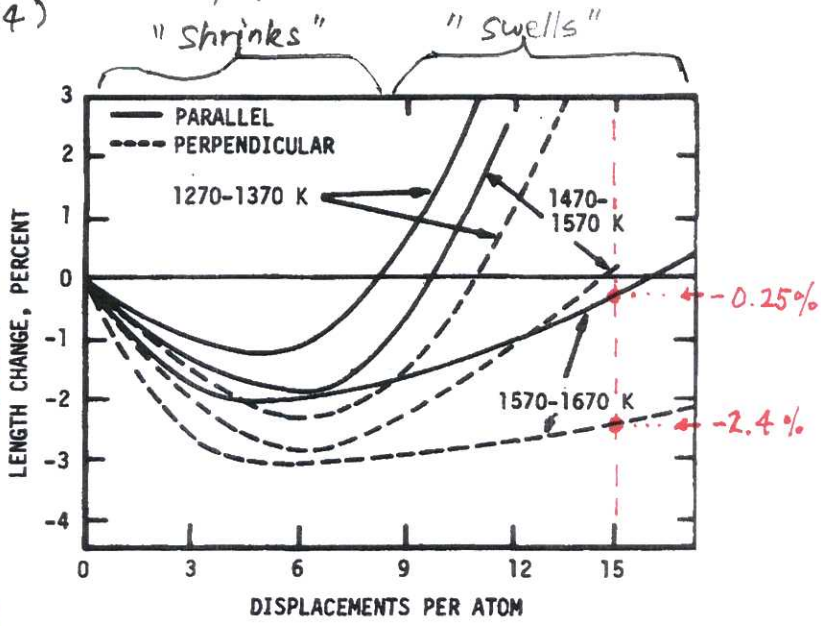

Fig. 8.34 Length changes of type 9,640 graphite parallel and perpendicular to the direction of molding as functions of the number of dpa (Kulcinski 1976)

Note: For graphite @ 1670°K
parallel $\frac{\Delta l}{l} \simeq -0.25\%$
and perpendicular $\frac{\Delta l}{l} \simeq -2.4\%$
@ 15 dpa
(≃ 1.9 MW/m² fluence)

- graphite suffers from chemical sputtering, absorbs tritium; however, at high temperatures (~ 1000 °C), tritium retention is significantly reduced; can endure to about 1-20 dpa.

8. Silicon Carbide (typical fiber thickness ~ 7-12 μm)

- not as good as graphite for thermal shock, but has better stability under neutron irradiation.

Table 8.13 Properties of silicon carbide composite (Chen et al. 2008; Snead et al. 2011)

Density ρ_m	kg/m^3	2,500
Porosity	%	10
Specific heat c_p	J/kg K	600
Poisson ratio		0.18
Thermal expansion coefficient α	K^{-1}	3E−6
Thermal conductivity k	W/m K	5–15
Young's modulus E	GPa	200
Electrical conductivity σ	$(\Omega\ m)^{-1}$	20

- SiC composite first wall with Pb Li coolant can endure up to 100 dpa/fpy (fpy = full power year) with a neutron wall load of 6 MW/m² and generate up to 10^4 appm (He)/fpy.

8. Silicon Carbide (cont'd)

Dolan, **Fig. 8.35** Fluence-dependent evolutions of swelling and thermal conductivity of carbon vapor deposited (CVD) SiC (Katoh et al. 2010)

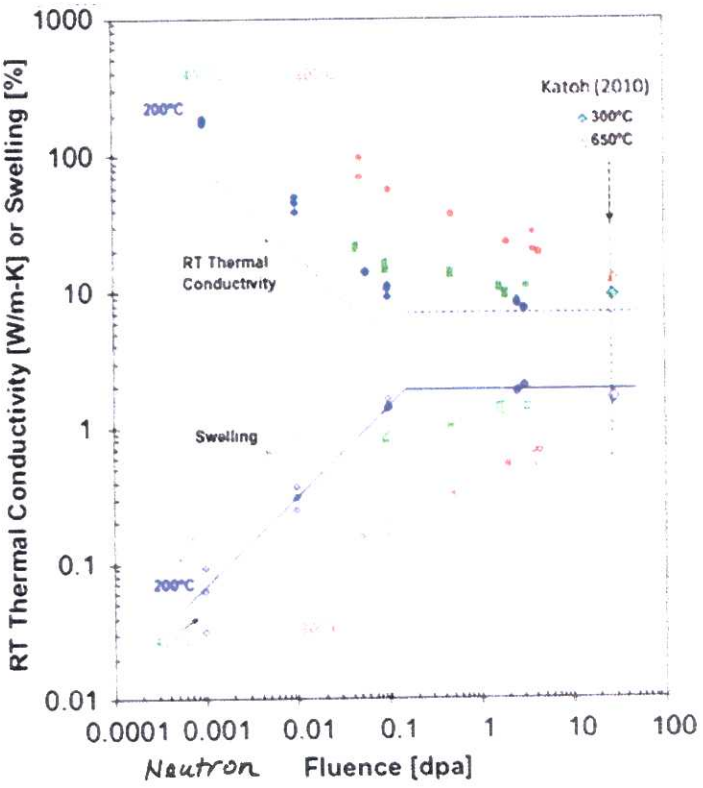

Note: At high temperature, e.g., 600-800 °C,
- thermal conductivity ↑ but
- swelling ↓

Table 8.15 Advantages and disadvantages of SiC

Advantages
Low decay heat
Low tritium trapping
Low radioactivity of pure SiC
Low chemical reactivity
Good electrical insulator
Disadvantages
Low thermal conductivity
Irradiation damage at high neutron fluences not quantified
Compatibility with PbLi uncertain at high temperatures

9. Copper

- stabilizes superconducting magnets and is used as substrate for actively-cooled plasma facing component (e.g., Be and W)

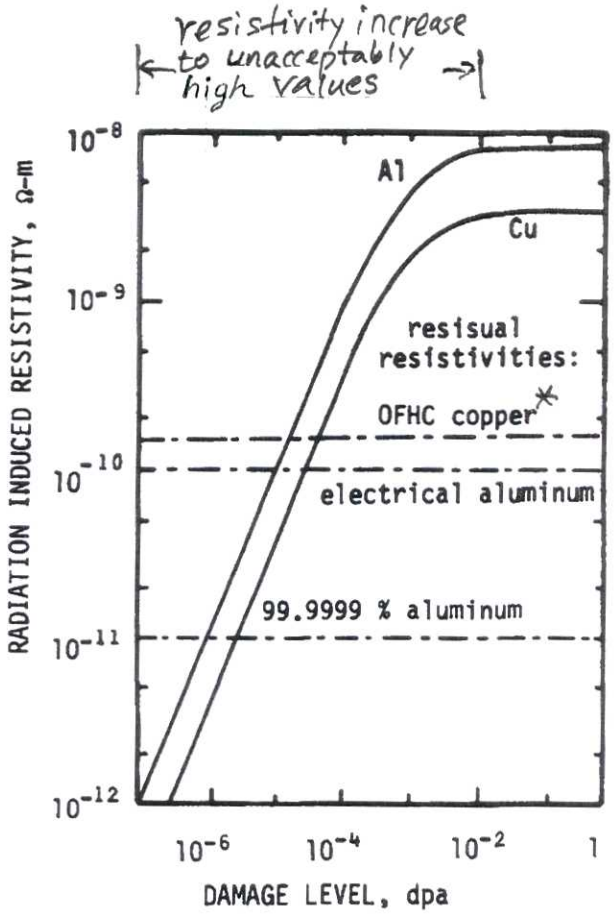

Dolan, **Fig. 8.36** Radiation-induced resistivities of aluminum and copper (Kulcinski 1976)

[* OFHC = Oxygen-free high thermal conductivity]

10. Superconducting Magnets

- NbTi has slight radiation damage effect;
- adequate shielding is required for Nb_3Sn due to the sensitivity of critical temperature at fluences around 10^{-3} dpa.
- radiation damage to the structure is not significant since the neutron fluence through superconducting coils is kept very low.

11. Liquid Metals (e.g., Ga, Sn, Li)

- good for use in high heat flux areas due to capabilities of high heat load and insensitivities to radiation damage; good for self-repair after a disruption.

Table 8.16 Properties of Ga, Sn, and Li (Majeski 2010)

Gallium
Z = 31, atomic weight = 69.7
Melting point = 29 8 °C, boiling point = 2,204 °C
Liquid density = 6. g cm^{-3}, sp. heat capacity = 0.37 J/g °C
Thermal conductivity: 40.6 W/m °C, electrical res. = 140 nΩ m
Vapor pressure = 10−7 Torr at 900 °C

Tin
Z = 50, atomic weight = 118.7
Melting point = 232 °C, boiling point = 2,602 °C
Liquid density = 7.0 g cm^{-3}, sp. heat capacity = 0.23 J/g °C
Thermal conductivity: 66.8 W/m °C, electrical res. = 115 nΩ m
Vapor pressure = 10−7 Torr at 1,000 °C

Lithium
Z = 3, atomic weight = 6.9
Melting point = 180.5 °C, boiling point = 1,342 °C
Liquid density = 0.5 g cm^{-3}, sp. heat capacity = 3.58 J/g °C
Thermal conductivity: 84.8 W/m °C, electrical res. = 93 nΩ m
Vapor pressure = 10−7 Torr at 400 °C
Hydrogen diffusivity ~ 10^{-4} cm^2/s

Good for high power reactors where recycling is not a problem; can operate at higher temperature

Can facilitate smaller fusion reactors

- PbLi is preferred over Li as breeder and coolant.

Dolan, **Fig. 8.38** Evaporation rates of Li, FLIBE, SnLi, Sn, and Ga versus temperature (Majeski 2010)

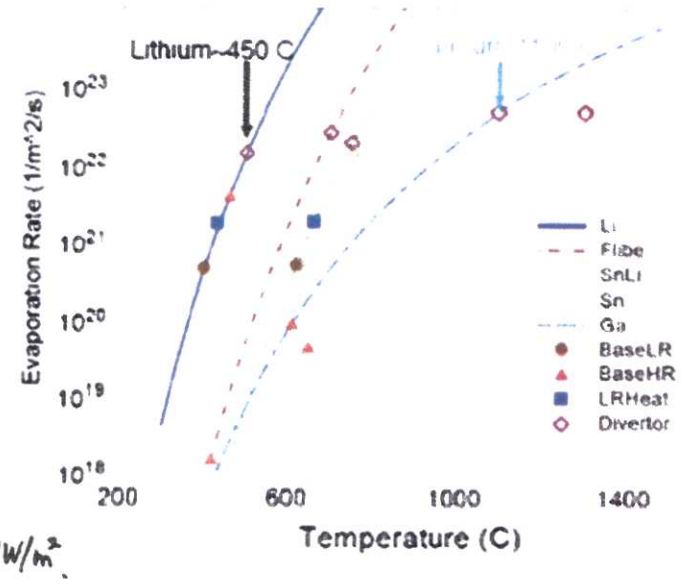

Note: FLIBE = Molten Salt ($LiF + BeF_2$)

Although high evaporation rate, Li accumulation in the core plasmas of many tokamaks is very little; required 5-10 m/s flow rate @ 2-5 MW/m^2.

Material Selection Considerations:

- Operating temperature ranges of some structural materials are considered below and the ODS (Oxide dispersion strengthened) ferritic steels and F/M (Ferritic/Martensitic - bcc) steels are preferred in Fig. 8.47 (below)

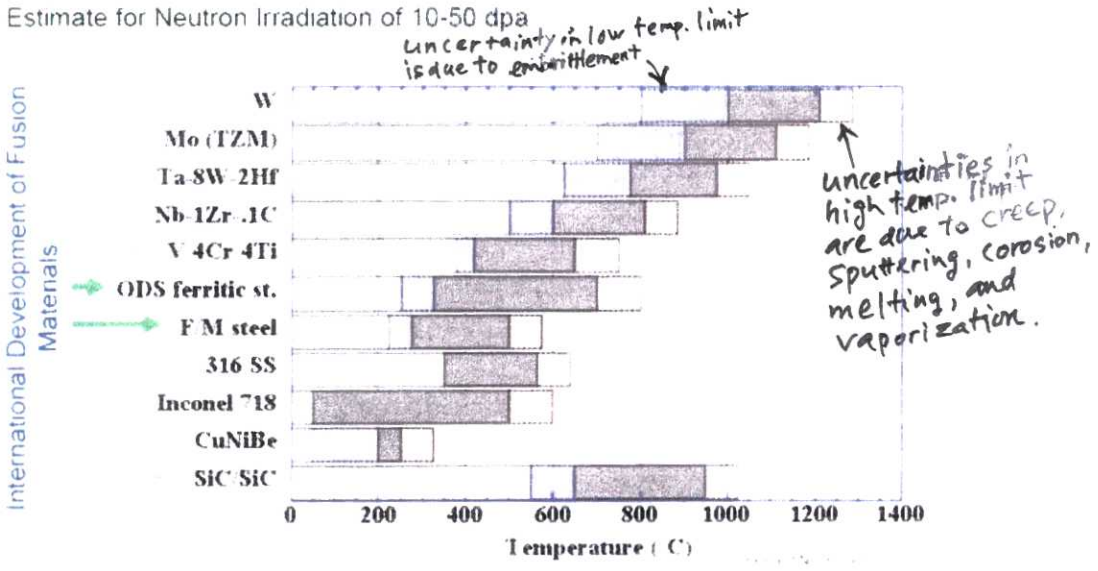

Fig. 8.47 Operating temperatures of some structural materials. Arrows indicate favored materials (Zinkle and Ghoniem 2000)